

HIP-2002-52/TH
 CERN-TH/2002-322
 hep-ph/0211239
 November 2002
 revised, March 2003

NONLINEAR CORRECTIONS TO THE DGLAP EQUATIONS IN VIEW OF THE HERA DATA

K.J. Eskola^{a,b,1}, H. Honkanen^{a,b,2}, V.J. Kolhinen^{a,b,3}, Jianwei Qiu^{c,4} and C.A. Salgado^{d,5}

^a *Department of Physics, University of Jyväskylä,
 P.O.Box 35, FIN-40014 University of Jyväskylä, Finland*

^b *Helsinki Institute of Physics,
 P.O.Box 64, FIN-00014 University of Helsinki, Finland*

^c *Department of Physics and Astronomy,
 Iowa State University, Ames, Iowa, 50011, U.S.A.*

^d *CERN, Theory Division, CH-1211 Geneva, Switzerland*

Abstract

The effects of the first nonlinear corrections to the DGLAP evolution equations are studied by using the recent HERA data for the structure function $F_2(x, Q^2)$ of the free proton and the parton distributions from CTEQ5L and CTEQ6L as a baseline. By requiring a good fit to the H1 data, we determine initial parton distributions at $Q_0^2 = 1.4 \text{ GeV}^2$ for the nonlinear scale evolution. We show that the nonlinear corrections improve the agreement with the $F_2(x, Q^2)$ data in the region of $x \sim 3 \cdot 10^{-5}$ and $Q^2 \sim 1.5 \text{ GeV}^2$ without paying the price of obtaining a worse agreement at larger values of x and Q^2 . For the gluon distribution the nonlinear effects are found to play an increasingly important role at $x \lesssim 10^{-3}$ and $Q^2 \lesssim 10 \text{ GeV}^2$, but rapidly vanish at larger values of x and Q^2 . Consequently, contrary to CTEQ6L, the obtained gluon distribution at $Q^2 = 1.4 \text{ GeV}^2$ shows a power-like growth at small x . Relative to the CTEQ6L gluons, an enhancement up to a factor ~ 6 at $x = 10^{-5}$, $Q_0^2 = 1.4 \text{ GeV}^2$ reduces to a negligible difference at $Q^2 \gtrsim 10 \text{ GeV}^2$.

¹kari.eskola@phys.jyu.fi

²heli.honkanen@phys.jyu.fi

³vesa.kolhinen@phys.jyu.fi

⁴jwq@iastate.edu

⁵carlos.salgado@cern.ch

1 Introduction

Parton distribution functions (PDFs), $f_i(x, Q^2)$, are needed for the computation of inclusive cross sections of hard, collinearly factorizable, processes in hadronic collisions. At sufficiently large values of the interaction scale Q^2 and the momentum fraction x , where power corrections are negligible, the scale evolution of the PDFs is predicted quite accurately by the Dokshitzer-Gribov-Lipatov-Altarelli-Parisi (DGLAP) evolution equations [1] derived from perturbative QCD.

In the global analyses of the PDFs of the free proton, such as in Refs. [2, 3], the lowest order (LO), next-to-leading order (NLO) and next-to-next-to-leading order (NNLO) parton distributions are extracted within the DGLAP framework using constraints from the measured cross sections of various hard processes and from the sum rules. In the proton case the procedure is well established: the initial distributions given at some initial scale Q_0^2 are first evolved to larger Q^2 by using the DGLAP equations, then a comparison with the data is made over a wide range of x and Q^2 , after which the initial distributions are iterated until a good global fit to the data is obtained. The initial distributions are thus the non-perturbative input needed, the element that perturbative QCD cannot predict. The data from deeply inelastic lepton-proton scattering (DIS) play a key role in these analyses especially in the region of the smallest values of x , where the DIS data from ep collisions at DESY-HERA give the only constraints available. Recently, the H1 collaboration at HERA [4] has measured the structure function $F_2(x, Q^2)$ of the proton down to $x \sim 3 \cdot 10^{-5}$ but still in the perturbatively accessible region $Q^2 \geq 1.5 \text{ GeV}^2$. These data have been included in the recent global analyses by the MRST [2] and CTEQ [3] collaborations.

In spite of the impressive success of the DGLAP approach, certain problems appear in the attempts to make the global fits to the H1 data [4] as good as possible *simultaneously* in the region of $Q^2 > 4 \text{ GeV}^2$ (“large” Q^2) and in the region of $1.5 \text{ GeV}^2 < Q^2 < 4 \text{ GeV}^2$ (“small” Q^2). In the recent NLO analysis MRST2001 [2] both regions are included and a good overall fit is found but with the expense of allowing for a negative gluon distribution. Although a negative contribution in the NLO gluon distribution is acceptable as long as the NLO cross sections remain positive, the interpretation of the PDFs as probability or number density distributions becomes obscured⁶. On the other hand, the CTEQ collaboration emphasizes the large- Q^2 region in their global fits: e.g. in the sets CTEQ5 [6] and CTEQ6 [3] only the region $Q^2 > 4 \text{ GeV}^2$ of the DIS data is included in the fit and a very good agreement with the data is found. The agreement of the extrapolation to the small- Q^2 region, however, becomes then worse. One is facing the problem of negative gluon distributions also in the NLO set CTEQ6M [3]: $xg(x, Q^2)$ is set to zero at the smallest values of x at scales $Q^2 \lesssim 1.69 \text{ GeV}^2$. In LO, the negative gluon distributions, however, are not allowed. The quality of the LO fits to the H1 data (see Table 1 in Sec. 3) reflects the problem of a simultaneous fit to the small- and large- Q^2 regions: MRST2001 (CTEQ6) fits the small- Q^2 (large- Q^2) region better.

The problems discussed above are very interesting as they can be a sign of a new QCD phenomenon: towards smaller values of x and (or) Q^2 (but still $Q^2 \gg \Lambda_{\text{QCD}}^2$), gluon recombination effects are expected to play an increasingly important role. These effects induce nonlinear power corrections to the DGLAP equations. First of the nonlinear terms have been calculated

⁶See also [5] for a recent discussion of the PDFs not being probabilities.

by Gribov, Levin and Ryskin in [7] and by Mueller and Qiu in [8]. We shall refer to these corrections as the GLRMQ terms.

Previous studies of the GLRMQ terms in the context of extracting the PDFs of the free proton can be found e.g. in [9]. Also other nonlinear evolution equations relevant at high gluon densities have been derived in the recent years [10], and the structure functions from DIS have been analysed in the context of saturation models [11]. In the present work, however, we shall adopt the framework of collinear factorization with universal PDFs, and search for the nonlinear GLRMQ corrections on top of the full DGLAP equations. This allows for a direct comparison of our results with those of the global DGLAP fits [2, 3]. In this manner we can also show more explicitly the need for nonlinear terms in the evolution equations.

In the DGLAP evolution, the Q^2 dependence of the sea quarks at small values of x is dictated by the gluon distribution: the larger $xg(x, Q^2)$, the faster the Q^2 evolution of $F_2(x, Q^2)$, since in LO $\partial F_2(x, Q^2)/\partial \log Q^2 \approx (10\alpha_s/27\pi)xg(2x, Q^2)$ [12]. The GLRMQ terms slow down the Q^2 evolution of gluons and sea quarks from the standard DGLAP behaviour (assuming the same starting distributions). Consequently, the $\log Q^2$ slopes of $F_2(x, Q^2)$ of the H1 data can be reproduced with a *larger* gluon distribution than that in the conventional DGLAP case. In this paper, we investigate this interdependence of the initial conditions at $Q_0^2 = 1.4 \text{ GeV}^2$ and the effects of the GLRMQ terms by using the H1 data as a baseline. We demonstrate that inclusion of the GLRMQ terms on top of the LO DGLAP evolution improves the agreement with the data in the small- x and small- Q^2 region while simultaneously maintains the good fit of the LO sets of CTEQ5 and CTEQ6 to the data at larger values of x and Q^2 . We show that the obtained small- x gluon distribution can still have a power-like growth at the scale $Q^2 = 1.4 \text{ GeV}^2$, leading to an enhancement of a factor ~ 6 relative to the CTEQ6L gluons at $x = 10^{-5}$. We also show explicitly how the large deviations from CTEQ6L reduce to very small differences at $Q^2 \gtrsim 10 \text{ GeV}^2$. The size of the nonlinear terms, uncertainties and applicability region of the DGLAP+GLRMQ approach are discussed as well.

2 Nonlinear evolution equations

The GLRMQ corrections [7, 8] arise from fusion of two gluon ladders, and they modify the evolution equations of gluons as

$$\frac{\partial xg(x, Q^2)}{\partial \log Q^2} = \frac{\partial xg(x, Q^2)}{\partial \log Q^2} \Big|_{\text{DGLAP}} - \frac{9\pi}{2} \frac{\alpha_s^2}{Q^2} \int_x^1 \frac{dy}{y} y^2 G^{(2)}(y, Q^2), \quad (1)$$

where the first term is the standard DGLAP result [1], linear in the PDFs. The 2-gluon density in the second term we model as

$$x^2 G^{(2)}(x, Q^2) = \frac{1}{\pi R^2} [xg(x, Q^2)]^2, \quad (2)$$

with $R = 1 \text{ fm}$ as the radius of the proton. The equation (1) thus becomes nonlinear in xg . In the scale evolution of the sea quark distributions the leading nonlinear correction from the gluon fusion appears as [8]

$$\frac{\partial xq(x, Q^2)}{\partial \log Q^2} \approx \left. \frac{\partial xq(x, Q^2)}{\partial \log Q^2} \right|_{\text{DGLAP}} - \frac{3\pi}{20} \frac{\alpha_s^2}{Q^2} x^2 G^{(2)}(x, Q^2), \quad (3)$$

where the first term is again from the DGLAP equations and linear in the PDFs. Note that here we work under an approximation of neglecting contribution from the “high twist” gluon distribution $G_{\text{HT}}(x, Q^2)$ [8]. More discussion on this will be given later [13]. The evolution of the valence quark distributions remains unmodified.

3 Analysis and Results

3.1 Effects of the GLRMQ corrections

The emphasis of the CTEQ analysis is in the large- Q^2 region where the nonlinearities should remain small. Since we wish to search for the nonlinear effects in the small- Q^2 (small- x) region but also recover the DGLAP evolution at large Q^2 , the CTEQ distributions are an ideal baseline for our analysis.

In Fig. 1, together with the H1 data [4], we plot the Q^2 dependence of the LO structure function $F_2(x, Q^2) = \sum_q e_q^2 [xq(x, Q^2) + x\bar{q}(x, Q^2)]$ computed from CTEQ5L [6, 14] for fixed values of x (dashed lines). The agreement with the H1 data is clearly getting worse towards smaller values of x and Q^2 . This trend is clearly visible also in Fig. 2 (dashed line), where we quantify the quality of the fit in terms of

$$\chi^2(x_k) = \sum_{x_j=0.2}^{x_k} \sum_{i=1}^{n(x_j)} \frac{[F_2^{\text{th}}(x_j, Q_i^{(x_j)}) - F_2^{\text{exp}}(x_j, Q_i^{(x_j)})]^2}{[\Delta_{F_2}^{\text{exp}}(x_j, Q_i^{(x_j)})]^2} \quad (4)$$

divided by the cumulative number of data points, $N(x_k) = \sum_{x_j=0.2}^{x_k} n(x_j)$, as a function of the x of the data. Here $n(x_j)$ refers to the number of the data points with the same value of $x = x_j$. The χ^2/N computed at different regions of Q^2 is in turn summarized in Table 1. Relative to the data [4] (which was not available at the time of CTEQ5) the computed $\log Q^2$ slopes of F_2 are too large at small values of x and Q^2 . This is caused by a too large gluon component in the DGLAP evolution at small values of x .

For showing how the GLRMQ terms slow down the scale evolution, we take the PDFs from the CTEQ5L parametrization at $Q^2 = 5 \text{ GeV}^2$, and evolve these both downwards and upwards by using the nonlinear evolution equations. The results are plotted in Fig. 1 (solid lines). As seen in the figure, at larger values of x and Q^2 the nonlinear effects remain small and do not make the agreement with the data worse. In addition, as shown both by Fig. 1 and Fig. 2, at $5 \cdot 10^{-5} \lesssim x \lesssim 10^{-3}$ the agreement with the data becomes quite good (i.e. χ^2/N remains constant), clearly improving the situation from the CTEQ5L case.

Another interesting observation from Fig. 1 is that, with the trial initial conditions above, the nonlinear corrections at $x \lesssim 5 \cdot 10^{-5}$ and $Q^2 \sim 1 \text{ GeV}^2$ obviously become too large and they start to dominate the computed evolution, causing negative $\log Q^2$ slopes for $F_2(x, Q^2)$. Clearly, these are not supported by the data. In the computation we would then have entered a gluon saturation region where also other correction terms in the evolution equations should be included. This region is thus beyond the scope of the present DGLAP+GLRMQ approach.

| | $Q^2 < 4.0 \text{ GeV}^2$ $N = 29$ | $Q^2 > 4.0 \text{ GeV}^2$ $N = 104$ | all Q^2 $N = 133$ |
|--|---------------------------------------|--|------------------------|
| CTEQ5L | 31.8 | 1.18 | 7.86 |
| CTEQ6L | 2.72 | 0.93 | 1.32 |
| MRST2001 | 0.59 | 2.06 | 1.74 |
| This work: | | | |
| Set 1: $Q_c < \sqrt{1.4} \text{ GeV}$ | 1.75 | 0.96 | 1.13 |
| Set 2a: $Q_c = 1.3 \text{ GeV}$ | 1.58 | 1.05 | 1.17 |
| Set 2b: $Q_c = \sqrt{1.4} \text{ GeV}$ | 0.95 | 0.86 | 0.88 |

Table 1: The χ^2/N of the fit of the computed LO F_2 to the H1 data [4] in the small- Q^2 and large- Q^2 regions. Also the number of data points in each case is mentioned.

The too strong nonlinearities can again be traced back to a too large gluon component at small x in the initial condition chosen. A more realistic gluon distribution which evolves according to the DGLAP+GLRMQ equations should obviously be smaller than CTEQ5L at small values of x at $Q^2 = 5 \text{ GeV}^2$.

The H1 data [4] is partly taken into account in the latest set CTEQ6L [3], and the situation is clearly improved from CTEQ5L. This is shown in Figs. 3 and 2 by the dotted-dashed curves. In Fig. 4 we have plotted the PDFs at $Q^2 = 1.4 \text{ GeV}^2$ for several cases. Now, as shown by Fig. 4, the gluon distributions (upper left panel) of CTEQ6L (dotted-dashed) at small x are smaller than those of CTEQ5L (dashed), causing more modest $\log Q^2$ slopes for F_2 at small x . Fig. 2 indicates that the agreement of CTEQ6L with the H1 data is excellent at $x \gtrsim 10^{-3}$ and stays very good also at smaller x . Table 1 again expresses χ^2/N at the large- Q^2 region (included in the CTEQ6 global fit) and in the small- Q^2 region (not included in the CTEQ6 fit). Although a good agreement with the data is found, a closer look at Fig. 3 shows that again the agreement of the pure DGLAP result is getting worse towards the smallest values of x .

We notice that, contrary to CTEQ5L, the CTEQ6L result in Fig. 3 lies above the H1 data at the smallest values of x . If we now simply took the initial conditions from CTEQ6L at, say, $Q^2 = 5 \text{ GeV}^2$, and evolved the distributions downwards by using the nonlinear equations (which would slow down the evolution), we would make the agreement with the data in the small- x region *worse* than the CTEQ6L result. The dotted curve in Fig. 2 shows the χ^2/N for such a run, notice the growing trend towards the smallest x . Encouraged, however, by the observations with the CTEQ5L+GLRMQ above, we wish to see whether we could find initial conditions at some Q_0^2 that would lead to at least the same or possibly even better agreement with the H1 data as the DGLAP result from CTEQ6L.

3.2 New initial distributions

3.2.1 Set 1

We construct the initial distributions at an initial scale $Q_0^2 = 1.4 \text{ GeV}^2$ by using the CTEQ5L and CTEQ6L sets as our guide. Following CTEQ5L we use $\Lambda_{\text{QCD}}^{(4)} = 192 \text{ MeV}$ together with the one-loop expression of the strong coupling constant. The change of the value of Λ_{QCD} at the heavy-quark mass thresholds is taken into account. Throughout the study we use $Q_b = 4.75 \text{ GeV}$ for the b -threshold, and the c -threshold will be discussed below. As seen in Fig. 2 (sparsely dotted curve), a good agreement with the H1 data is found at $x \gtrsim 0.01$ by taking the CTEQ6L PDFs at 5.0 GeV^2 and evolving them down to 1.4 GeV^2 according to the nonlinear equations. The CTEQ5L distributions evolved down to 1.4 GeV^2 from 10.0 GeV^2 and 3.0 GeV^2 with the GLRMC corrections included, give a reasonably good agreement with the H1 data at $10^{-4} \lesssim x \lesssim 0.01$ and at $10^{-5} \lesssim x \lesssim 10^{-4}$, correspondingly (not shown). A working initial condition can then be found by interpolating between these three results. Finally, we make a power-law fit to the interpolated gluon and light sea-quark distributions at small values of x . The x -slope of the small- x gluons is tuned to reproduce the measured $\log Q^2$ slopes of F_2 . This leads to an initial gluon distribution $xg(x, Q_0^2) = 3.64 \cdot (0.01/x)^{0.28}$ at small x .

The initial conditions constructed in this way at $Q_0^2 = 1.4 \text{ GeV}^2$ are shown in Fig. 4, labelled as our “set 1”. The obtained distributions are compared with the CTEQ5L and CTEQ6L PDFs at the same scale. Notice especially that our gluon distribution at $x = 10^{-5}$ at this scale is a factor 6.4 larger than the one in CTEQ6L. In turn, the light sea-quark distributions at small x lie in between CTEQ6L and CTEQ5L. Due to the procedure we have chosen, the valence-quark distributions (which evolve according to DGLAP) are practically the same as in CTEQ5L at $x \lesssim 0.01$ and CTEQ6L at $x \gtrsim 0.01$.

The DGLAP+GLRMC evolution to higher scales then gives the result shown in Fig. 3 by the solid lines. The corresponding values of χ^2/N are again shown as a function of x in Fig. 2 and its division into small- Q^2 and large- Q^2 regions in Table 1. We observe that while the agreement with the H1 data at large values of x and Q^2 is maintained practically as good as in CTEQ6L, the fit in the smallest- x , small- Q^2 region is indeed improving. This, together with the parton distributions at $Q_0^2 = 1.4 \text{ GeV}^2$ for the nonlinear evolution, is the main result of this paper. At this point we should also emphasize that we have not attempted to make a global statistical analysis such as the one by CTEQ in order to further minimize the χ^2 . After such a procedure, further improvement on the χ^2 could well be anticipated.

Fig. 5 shows the Q^2 dependence of the gluon distributions at fixed values of x as obtained in the DGLAP analyses CTEQ5L (dashed lines) and CTEQ6L (dotted-dashed) as well as from the GLRMC+DGLAP evolution of the gluons of our set 1 (solid). Notice on one hand the large difference in the CTEQ5L and CTEQ6L sets, and on the other hand the slower evolution in the nonlinear case at small values of x and Q^2 . We also draw attention to the fact that in spite of the large (factor 6.4) difference at $Q_0^2 = 1.4 \text{ GeV}^2$ at $x = 10^{-5}$, our gluon distributions and the CTEQ6L gluons are in fact quite similar at $Q^2 \gtrsim 5 \text{ GeV}^2$. Coming back to the discussion related to Fig 1, we also observe from Fig. 5 that at $Q^2 = 5 \text{ GeV}^2$ the gluons from our set 1 are below the CTEQ5L gluons as anticipated.

3.2.2 Sets 2a and 2b

A detail to study next is the c -quark contribution. The initial distributions in our set 1 were obtained on the basis of distributions which were evolved downwards from 3, 5 and 10 GeV² according to the nonlinear evolution equations. The c -quarks we treat as massless quarks which experience the GLRMQ corrections as well. Therefore, the downwards evolution of the c -quarks is also slower than in the DGLAP case, and their distributions vanish only somewhat below the threshold scale $Q_c = 1.3$ GeV of the sets CTEQ6L and CTEQ5L. This explains the fairly large c -distribution at Q_0^2 in our set 1.

We construct two slightly different sets of PDFs with the same initial conditions at $Q_0^2 = 1.4$ GeV², where $xc(x, Q_0^2) = 0$. For the first case, called “set 2a” we follow CTEQ6L and take $Q_c = 1.3$ GeV as the c -threshold scale. For the other case, called “set 2b” we choose, $Q_c = Q_0 = \sqrt{1.4}$ GeV. In these initial conditions, the gluons are not modified from set 1. However, in order to compensate for the loss of the initial c -quarks and to recover the agreement with the H1 data, we enhance the other sea-quarks in the small- x region simply by tuning their power in the power-law fit. The initial distributions for our sets 2 are shown in Fig. 4 (double dashed). After the nonlinear evolution to higher scales, the agreement of the set 2a with the H1 data is practically as good as with our set 1 and CTEQ6L, as is shown in Figs. 3 and 2 (double dashed lines). With the set 2b, the agreement becomes even better, as can be seen from Figs. 2 and 3 (short dashed lines). The same conclusion is suggested also by the χ^2/N computed in the different regions of Q^2 in Table 1. The GLRMQ corrections thus improve the fits to the data in the region of small x and Q^2 without losing the good fits at larger x and Q^2 . Regarding the sensitivity of the results to the c -threshold, we note that the differences between our sets 2a and 2b are quite small and could most probably be obtained also by keeping the c -threshold constant while tuning the gluon distributions at $0.001 \lesssim x \lesssim 0.01$. This fine-tuning is, however, beyond the goal of this paper.

4 Discussion and Conclusions

It is important to keep in mind the uncertainties and limitations of the present approach. A constraint not addressed above but used in the global analysis of the PDFs, is momentum conservation. Due to the nonlinear terms in Eqs. (1) and (3), some momentum from small values of x is lost in the evolution towards higher scales. Due to this, our sets 1 and 2 overestimate the total momentum at $Q_0^2 = 1.4$ GeV² by less than 2 %. By $Q^2 = 100$ GeV², some 2.6 % of the initial total momentum is lost. As the emphasis of our study is in the small- x behaviour of the PDFs, and as the violation remains small, we have not made an attempt to correct the obtained distributions for the momentum sum rule.

In modelling the 2-gluon density in Eq. (1), we have set the effective radius parameter of the free proton to $R = 1$ fm. Depending on the transverse matter density profile assumed for the free proton, some ~ 20 % uncertainty in R can be expected. The nonlinearities decrease with increasing R , so due to the interplay between the initial conditions and the scale evolution demonstrated above, a larger R would lead to a smaller enhancement of the small- x gluons. In order to properly estimate the uncertainty in the initial gluon distribution caused by the uncertainty in R , the fit analysis performed above should be redone with modified values of R .

While this is beyond the scope of the present paper, it is left as a future task.

The form $\sim (xg)^2$ for the 2-gluon density also neglects possible longitudinal correlations which should suppress the 2-gluon density at sufficiently large values of x . Also the possible difference of the fractional momenta of the fusing gluons is neglected. It can be argued, based on a simple picture of a Lorentz contracted proton and wavelengths of partons given by their inverse momentum, that gluons with $x < 1/(2m_p R) \sim 0.1$ overlap with any other gluons and thus cause finite nonlinear corrections. As the 1-gluon densities are already decreasing quite rapidly at $x \gtrsim 0.1$, and as their $\log Q^2$ slopes become anyway small there, we have not attempted to build in any longitudinal correlations of the fusing gluons. In a larger system, in a big nucleus, this would be necessary, and sensitivity to such details should be studied.

Another obvious improvement for the present analysis is to consider the GLRMQ terms added on top of the NLO DGLAP evolution. In that case, the zero (CTEQ6M) or negative (MRST2001) gluon distributions at small x may become larger than zero.

In the present study we have neglected a possible but small contribution from the higher-dimensional gluon distribution G_{HT} introduced in [8]. The distribution G_{HT} can be thought as a k_T^2 moment of k_T -dependent gluon distribution, and its upper limit estimated as $G_{HT}(x, Q^2) \approx \langle k_T^2 \rangle g(x, Q^2) < Q^2 g(x, Q^2)$. Therefore, this term should be less than the normal DGLAP term, and remain negligible. Further studies on this interesting question will follow [13].

Regarding the size of the nonlinear terms, it is quite interesting to notice that in our results at $Q_0^2 = 1.4 \text{ GeV}^2$, the GLRMQ terms in Eq. (1) make about 48 % of the full DGLAP+GLRMQ $\log Q^2$ slope of the gluon distribution at $x = 10^{-5}$, and still some 16% at $x = 0.01$. The extent of nonlinearity decreases, as expected, with increasing Q^2 : at $Q^2 = 10 \text{ GeV}^2$ the GLRMQ contribution to the total $\partial xg/\partial \log Q^2$ is 26 % at $x = 10^{-5}$ and below 4% at $x = 0.01$. At the lowest values of Q^2 and x probed by the H1 data [4], we clearly are at the borderline of the applicability of the approach, i.e. close to the gluon saturation region, where the next terms in the nonlinear evolution equations are becoming important [15, 16, 17, 18]. The further nonlinear correction terms obviously enter with an alternating sign. In the region where the GLRMQ term in Eqs. (1) and (3) becomes as important as the DGLAP term, inclusion of the further corrections should thus decrease the net correction. Therefore, the results of the current paper in the region of smallest x and Q^2 studied can be regarded as an upper limit of the small- x gluon distributions.

In conclusion, we have studied the effects of adding the nonlinear GLRMQ corrections to the LO DGLAP evolution equations, and especially the interplay between the initial conditions and the nonlinearities. We use the PDF sets CTEQ5L and CTEQ6L as a baseline, and the recent DIS data from H1 [4] as a constraint. We have shown that the agreement between the measured and computed structure function $F_2(x, Q^2)$ can be improved at small values of x and Q^2 while still maintaining the good fit to the data obtained in the global analyses at larger values of x and Q^2 . The nonlinearities slow down the scale evolution, so in order to recover the measured $\log Q^2$ slopes of $F_2(x, Q^2)$ of the data, a larger small- x gluon distribution than that in CTEQ6L is needed. For the gluon distribution the nonlinear effects are found to play an increasingly important role at $x \lesssim 10^{-3}$ and $Q^2 \lesssim 10 \text{ GeV}^2$. The nonlinearities, however, vanish rapidly at larger values of x and Q^2 . Consequently, contrary to CTEQ6L, the obtained gluon distribution at $Q^2 = 1.4 \text{ GeV}^2$ shows a power-like growth at small values of x . Relative to the CTEQ6L gluons, an enhancement up to a factor ~ 6 at $x = 10^{-5}$, $Q^2 = 1.4 \text{ GeV}^2$ reduces to a

negligible difference at $Q^2 \gtrsim 10 \text{ GeV}^2$.

Acknowledgements. We thank N. Armesto, P.V. Ruuskanen, I. Vitev and other participants of the CERN Hard Probes workshop for discussions. We are grateful for the Academy of Finland, Project 50338, for financial support. J.W.Q. is supported in part by the United States Department of Energy under Grant No. DE-FG02-87ER40371. C.A.S. is supported by a Marie Curie Fellowship of the European Community programme TMR (Training and Mobility of Researchers), under the contract number HPMF-CT-2000-01025.

References

- [1] Yu. Dokshitzer, Sov. Phys. JETP **46** (1977) 1649; V.N. Gribov and L. N. Lipatov, Sov. Nucl. Phys. **15** (1972) 438, 675; G. Altarelli, G. Parisi, Nucl. Phys. B **126** (1977) 298.
- [2] A. D. Martin, R. G. Roberts, W. J. Stirling and R. S. Thorne, Eur. Phys. J. C **23** (2002) 73 [arXiv:hep-ph/0110215]; Phys. Lett. B **531** (2002) 216 [arXiv:hep-ph/0201127].
- [3] J. Pumplin *et al.*, arXiv:hep-ph/0201195.
- [4] C. Adloff *et al.* [H1 Collaboration], Eur. Phys. J. C **21** (2001) 33 [arXiv:hep-ex/0012053].
- [5] S. J. Brodsky, P. Hoyer, N. Marchal, S. Peigne and F. Sannino, Phys. Rev. D **65** (2002) 114025 [arXiv:hep-ph/0104291].
- [6] H. L. Lai *et al.* [CTEQ Collaboration], Eur. Phys. J. C **12** (2000) 375 [arXiv:hep-ph/9903282].
- [7] L. V. Gribov, E. M. Levin and M. G. Ryskin, Phys. Rept. **100** (1983) 1.
- [8] A. H. Mueller and J. Qiu, Nucl. Phys. B **268** (1986) 427.
- [9] J. Kwiecinski, A. D. Martin, W. J. Stirling and R. G. Roberts, Phys. Rev. D **42** (1990) 3645.
- [10] A. H. Mueller, Nucl. Phys. **B335** (1990) 115; **B558** (1999) 285; L. McLerran and R. Venugopalan, Phys. Rev. **D49** (1994) 2233; 3352; **D50** (1994) 2225; I. I. Balitsky, Nucl. Phys. **B463** (1996) 99. Yu. V. Kovchegov, Phys. Rev. **D54** (1996) 5463; J. Jalilian-Marian, A. Kovner, L. McLerran and H. Weigert, Phys. Rev. **D55** (1997) 5414; Yu. V. Kovchegov and A. H. Mueller, Nucl. Phys. **B529** (1998) 451; **D55** (1997) 5445; M. A. Braun, Eur. Phys. J. **C16** (2000) 337; E. Iancu, A. Leonidov and L. McLerran, Nucl. Phys. **A692** (2001) 583; A. Kovner and U. A. Wiedemann, Phys. Rev. D **64** (2001) 114002.
- [11] K. Golec-Biernat and M. Wusthoff, Phys. Rev. D **59** (1999) 014017; W. Buchmuller, T. Gehrmann and A. Hebecker, Nucl. Phys. B **537** (1999) 477, E. Gotsman, E. Ferreira, E. Levin, U. Maor and E. Naftali, Phys. Lett. B **500** (2001) 87; J. Bartels, K. Golec-Biernat and H. Kowalski, Phys. Rev. D **66** (2002) 014001; E. Gotsman, E. Levin, M. Lublinsky and U. Maor, arXiv:hep-ph/0209074.

- [12] K. Prytz, Phys. Lett. **B311** (1993) 286.
- [13] K. J. Eskola *et al.*, in preparation.
- [14] H. Plathow-Besch, Comp. Phys. Comm. 75 (1993) 396; Int. J. Mod. Phys. **A10** (1995) 2901; “PDFLIB: Proton, Pion and Photon Parton Density Functions, Parton Density Functions of the Nucleus, and α_s ”, Users’s Manual - Version 8.04, W5051 PDFLIB 2000.04.17 CERN-ETT/TT.
- [15] A. L. Ayala, M. B. Gay Ducati and E. M. Levin, Nucl. Phys. B **493** (1997) 305 [arXiv:hep-ph/9604383].
- [16] J. Jalilian-Marian and X. N. Wang, Phys. Rev. D **60** (1999) 054016 [arXiv:hep-ph/9902411].
- [17] H. Weigert, Nucl. Phys. A **703** (2002) 823 [arXiv:hep-ph/0004044].
- [18] Y. V. Kovchegov and K. Tuchin, Phys. Rev. D **65** (2002) 074026 [arXiv:hep-ph/0111362].

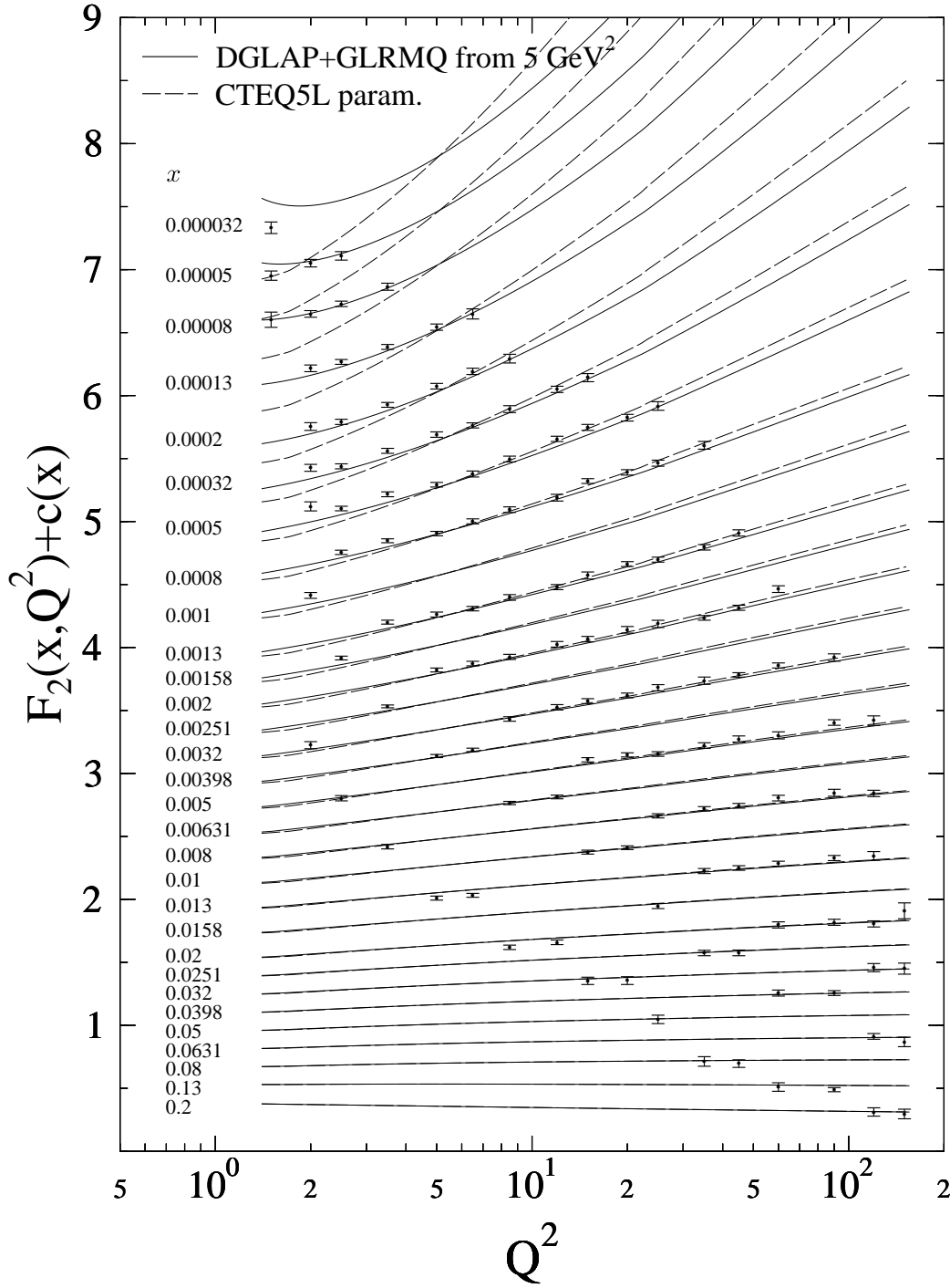


Figure 1: The scale evolution of the structure function $F_2(x, Q^2)$ of the free proton for fixed values of x (with constants added to separate the curves). The dashed curves show the LO DGLAP result from CTEQ5L [6], and the solid curve the result after the DGLAP+GLRMQ evolution when initial conditions taken from CTEQ5L at $Q_0^2 = 5 \text{ GeV}^2$. The data is from H1 [4] and the error bars are statistical.

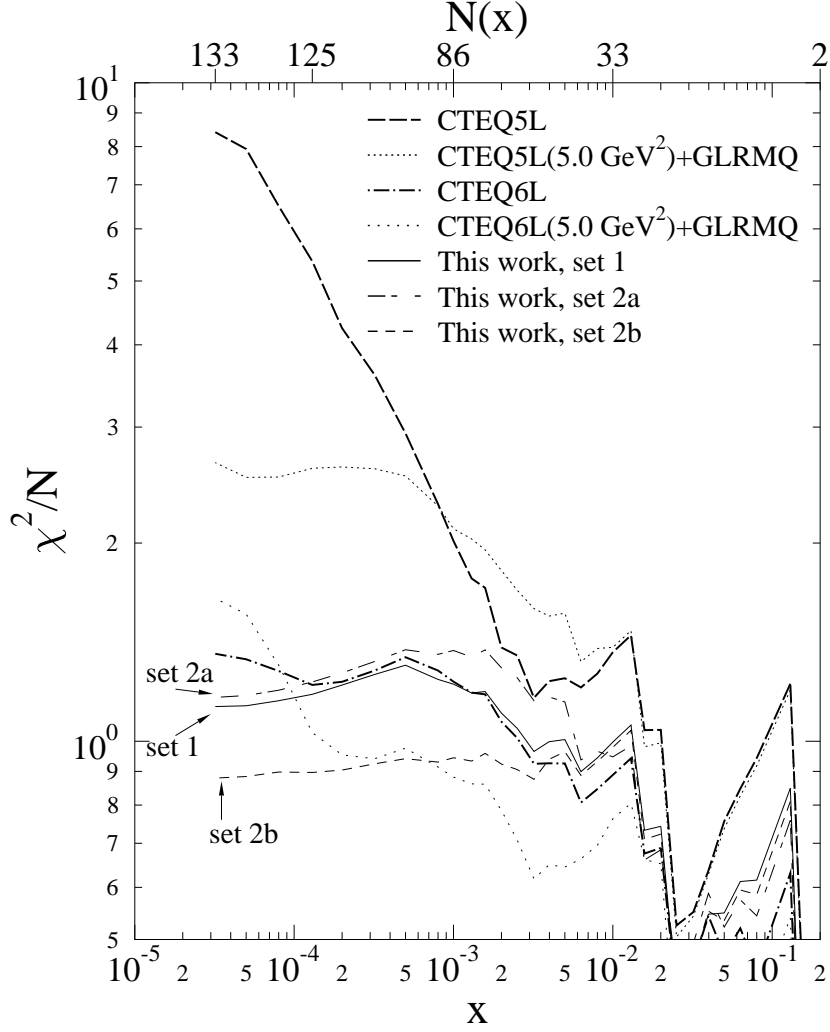


Figure 2: The goodness parameter χ^2 of the fits of the computed $F_2(x, Q^2)$ to the H1 data, divided by the number of data points, as a function of the x of the data. The cumulative number of the data points is increasing to the left as indicated at the top of the plot: $N(x = 0.2) = 2$ and $N(x = 3.2 \cdot 10^{-5}) = 133$ (see also Table 1). The curves are the LO DGLAP results from CTEQ5L (long dashed thick line) and CTEQ6L (dotted-dashed thick line), the DGLAP+GLRMQ result with the initial conditions at $Q^2 = 5 \text{ GeV}^2$ taken from CTEQ5L (densely dotted) and from CTEQ6L (sparsely dotted), and, our set 1 (solid), set 2a (double dashed) and set 2b (short dashed) .

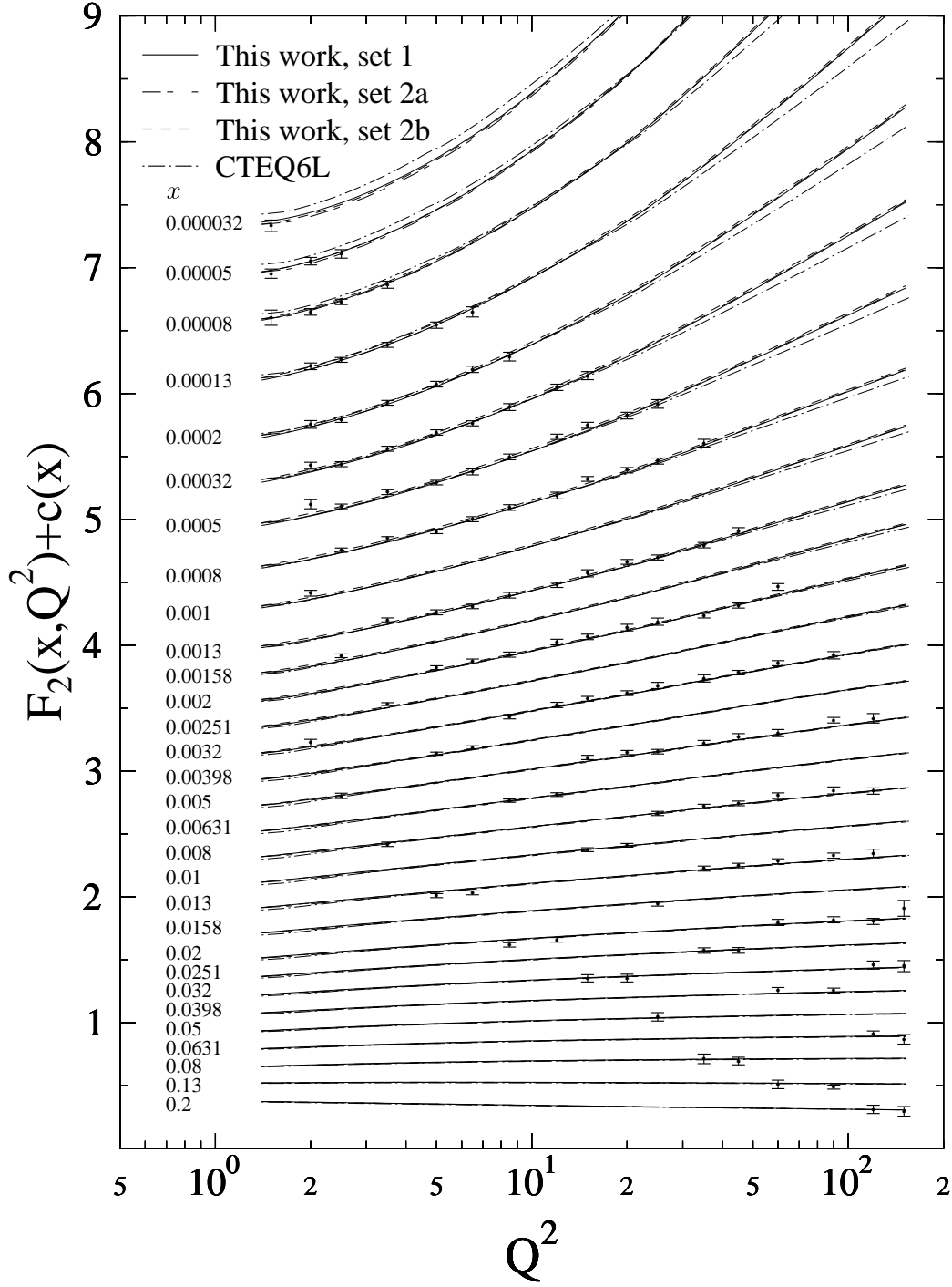


Figure 3: As Fig. 1 but for LO DGLAP result from CTEQ6L (dotted-dashed) and for the DGLAP+GLRQM results with our set 1 (solid), set 2a (double dashed) and set 2b (short dashed).

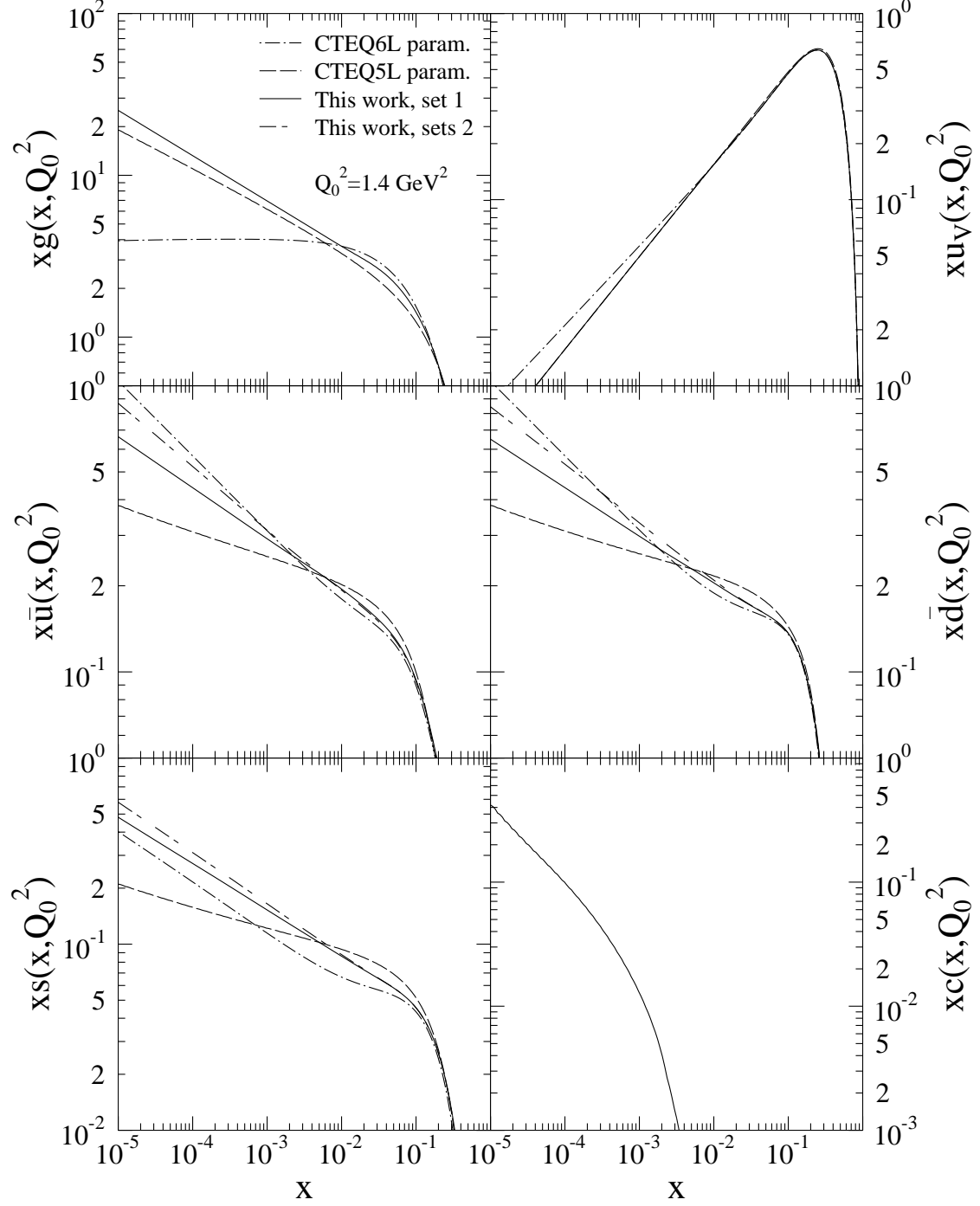


Figure 4: The parton distribution functions at $Q^2 = 1.4 \text{ GeV}^2$ as obtained in the DGLAP analyses CTEQ5L [6] (dashed), CTEQ6L [3] (dotted-dashed) and in the present work based on the DGLAP+GLRMQ evolution. In our set 1 (solid), there is a finite charm contribution, while in the sets 2 (double dashed) charm is zero at this scale. Notice the enhancement from the CTEQ6L glue. The gluon distributions of set 1 and sets 2 are identical.

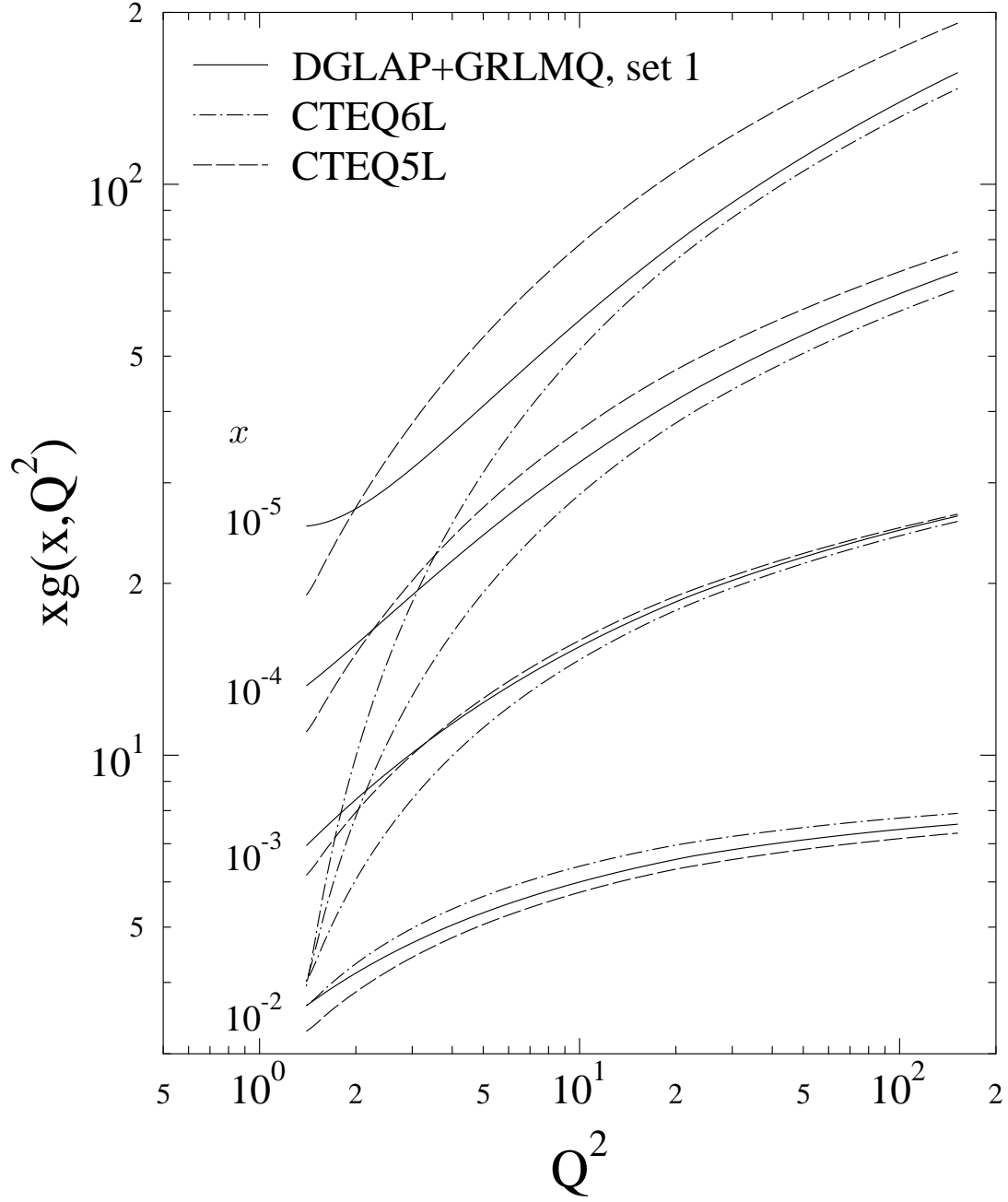


Figure 5: The Q^2 dependence of the gluon distribution function at fixed values of x , from CTEQ5L [6] (dashed), CTEQ6L [3] (dotted-dashed) and set 1 of the present work (solid). Notice the logarithmic scales and the absolute normalization of the curves.